[CANCER RESEARCH 61, 7754–7762, November 1, 2001]

Polyamine Depletion in Human Melanoma Cells Leads to G_1 Arrest Associated with Induction of $p21^{WAF1/CIP1/SDI1}$, Changes in the Expression of p21-regulated Genes, and a Senescence-like Phenotype[1]

Debora L. Kramer, Bey-Dih Chang, Ying Chen, Paula Diegelman, Kersti Alm, Adrian R. Black, Igor B. Roninson, and Carl W. Porter[2]

Grace Cancer Drug Center, Roswell Park Cancer Institute, Elm and Carlton Streets, Buffalo, New York 14263 [D. L. K., Y. C., P. D., K. A., A. R. B., C. W. P.], and Department of Molecular Genetics, University of Illinois at Chicago, Chicago, Illinois 60607-7170 [B-D. C., I. B. R.]

ABSTRACT

The cell cycle regulatory events that interface with polyamine requirements for cell growth have not yet been clearly identified. Here we use specific inhibitors of polyamine biosynthetic enzymes to investigate the effect of polyamine pool depletion on cell cycle regulation. Treatment of MALME-3M cells with either the ornithine decarboxylase inhibitor α-difluoromethylornithine or the *S*-adenosylmethionine decarboxylase inhibitor MDL-73811 lowered specific polyamine pools and slowed cell growth but did not induce cell cycle arrest. By contrast, treatment with the combination of inhibitors halted cell growth and caused a distinct G_1 arrest. The latter was associated with marked reduction of all three polyamine pools, a strong increase in $p21^{WAF1/CIP1/SDI1}$ (p21), and hypophosphorylation of retinoblastoma protein. All effects were fully prevented by exogenous polyamines. p21 induction preceded p53 stabilization in MALME-3M cells and also occurred in a polyamine-depleted, p53-nonfunctional melanoma cell line, indicating that p21 is induced at least in part through p53-independent mechanisms. Conditional overexpression of p21 in a fibrosarcoma cell line was shown previously to inhibit the expression of multiple proliferation-associated genes and to induce the expression of genes associated with various aspects of cell senescence and organism aging. Polyamine depletion in MALME-3M cells was associated with inhibition of seven of seven tested p21-inhibited genes and with induction of 13 of 14 tested p21-induced genes. p21 expression is also known to induce a senescence-like phenotype, and phenotypic features of senescence were observed in polyamine-depleted MALME-3M cells. Cells increased in size, appeared more granular, and expressed senescence-associated β-galactosidase. Cells released from the polyamine inhibition lost the ability to form colonies, failed to replicate their DNA, and ~25% became bi- or multinucleated. These events parallel the outcome of prolonged p21 induction in fibrosarcoma cells. The results of this study indicate that polyamine pool depletion achieved by specific biosynthetic enzyme inhibitors causes p21-mediated G_1 cell cycle arrest followed by p21-mediated changes in gene expression, development of a senescence-like phenotype, and loss of cellular proliferative capacity.

INTRODUCTION

It is well established that selective pharmacological interference with the synthesis of natural polyamines results in tumor cell growth inhibition under both *in vitro* and *in vivo* conditions (1, 2). Dramatic increases in the activity of the sentinel polyamine biosynthetic enzyme ODC[3] have been linked to the G_1-S transition (3–5). An apparent molecular basis for this derives from the fact that ODC is among those genes known to be transactivated by c-*myc* and N-*myc* (6–8), oncogenic transcription factors known to regulate entry into and exit from the cell cycle. To date, the requirement for polyamines in cell cycle progression has been variably defined with some reports indicating a role in G_1-S transition (9–12), others, a role in the S and/or G_2 phases of the cell cycle (13–15), and still others suggesting a general lengthening of all phases of the cycle (16). This lack of literature consensus is at least partially attributable to differences in the cell type being studied, the enzyme being inhibited, and/or the variable specificity of the inhibitors being used. In addition, there are certain technical difficulties imposed by the time required to deplete natural polyamines with single enzyme inhibitors.

Recently we examined the cell cycle effects of DENSPM, a clinically evaluated polyamine analogue (17), thought to inhibit cell growth by disrupting intracellular polyamine pool homeostasis (18–20). By creating an intracellular state of apparent polyamine excess, the analogue down-regulates polyamine biosynthesis and uptake while at the same time potently up-regulating polyamine catabolism as indicated by massive increases in Spd/Spm N^1-acetyltransferase activity. The net result is a rapid and near total depletion of intracellular polyamine pools and their replacement with the dysfunctional analogue (17). With respect to the cell cycle, DENSPM and related analogues cause G_1 and G_2-M arrests followed by a delayed apoptotic response in MALME-3M human melanoma cells (21). The G_1 arrest is accompanied by an early induction of p53, cdk inhibitor p21, and hypophosphorylation of Rb checkpoint. Because these effects did not occur in human melanoma cells containing a mutated form of p53 (22), it is not clear whether the response to analogues is attributable to events related to apparent polyamine excess or to the resulting depletion of natural polyamines.

Induction of specific cell cycle proteins provides a sensitive and early end point for studying the role of polyamines in cell proliferation. The present investigation was undertaken to define the cell cycle effects and associated protein responses to polyamine pool depletion. In an earlier paper, Ray *et al.* (23) reported modest increases in p21, p27, and p53 in IEC-6 intestinal epithelial cells treated with DFMO. However, the sequence of induction of the various proteins and their temporal relevance to the onset of G_1 arrest or to depletion of intracellular polyamine pools was not investigated. In the absence of

Received 1/8/01; accepted 9/4/01.

The costs of publication of this article were defrayed in part by the payment of page charges. This article must therefore be hereby marked *advertisement* in accordance with 18 U.S.C. Section 1734 solely to indicate this fact.

[1] Supported in part by National Cancer Institute Grants RO1 CA-22153 (to C. W. P.), CA-62099, and CA-89636 (to I. B. R.); grants from the American Cancer Society, Illinois Division, and the American Foundation for Alternatives to Animal Research (to B-D. C.); and Institute Core Grant CA-16056. Dr. Kersti Alm, a visiting postdoctoral fellow in the laboratory of C. W. P., was supported by a Research Training Fellowship awarded by the International Agency for Research on Cancer.

[2] To whom requests for reprints should be addressed, at Grace Cancer Drug Center, Roswell Park Cancer Institute, Elm and Carlton Streets, Buffalo, NY 14263. Phone: (716) 845-3002; Fax: (716) 845-2353; E-mail: Carl.Porter@roswellpark.org.

[3] The abbreviations used are: ODC, ornithine decarboxylase; βAPP, β-amyloid precursor protein; cdk, cyclin-dependent kinase; DENSPM, N^1, N^{11}-diethylnorspermine also known as DE-333 or BENSPM as in N^1, N^{11}-bis(ethyl)norspermine; MDL-73811, 5′-5′-{[(Z)-4-amino-2-butenyl]methylamino}-5′-deoxy-adenosine also known as AbeAdo; DFMO, α-difluoromethylornithine also known as Eflornithine; DHFR, dihydrofolate reductase; FM, drug-free medium; Mac2-BP, Mac2-binding protein; PAI-1, plasminogen activator inhibitor; p16, $p16^{Ink4A}$; p21, $p21^{WAF1/CIP1/SDI1}$; p27, $p27^{Kip1}$; Put, putrescine; Rb, retinoblastoma protein; ppRb, hyperphosphorylated Rb; pRb, hypophosphorylated Rb; RT-PCR, reverse transcription-polymerase chain reaction; SAMDC, *S*-adenosylmethionine decarboxylase; SA-β-gal, senescence-associated β-galactosidase; β-gal, β-galactosidase; SOD2, manganese superoxide dismutase; Spd, spermidine; BrdUrd, bromodeoxyuridine; Spm, spermine; t-Tgase, tissue transglutaminase; TS, thymidylate synthase; Topo IIα, topoisomerase IIα.

multiple early time point measurements, a causal role of p53 or the cdk inhibitors could not be deduced. In another study, Li *et al.* (24) reported that DFMO treatment of IEC-6 cells resulted in significant increases in p53 expression and G_1 arrest in the absence of apoptosis. Because p53 measurements were conducted well after G_1 arrest had been established, the relationship between p53 expression and growth arrest was, again, uncertain. Such distinctions are important in defining the upstream functional interface of polyamine pool depletion with the cell cycle regulatory pathways.

In this present study, we use a combination of specific ODC and SAMDC inhibitors to sharpen induction of cell cycle arrest and thereby facilitate investigation of underlying regulatory responses. Our findings indicate a close temporal association between polyamine pool depletion and G_1 arrest related to induction of p21 with subsequent hypophosphorylation of Rb. p21 induction in polyamine-depleted cells is followed by a complex set of changes in cell morphology and gene expression, which reproduce to a surprising degree the effects observed previously of p21 expression from an inducible promoter in HT1080 fibrosarcoma cells. More particularly, these p21-mediated changes include the development of phenotypic features of cell senescence and irreversible loss of proliferative capacity after polyamine depletion.

MATERIALS AND METHODS

Materials. The ODC inhibitor DFMO (Fig. 1) was provided by ILEX Inc. (San Antonio, TX) and the SAMDC inhibitor, MDL-73811 (25) by Aventis Pharmaceuticals Inc. (Bridgewater, NJ). The polyamines, Hoechst dye (33342), and BrdUrd were obtained from Sigma Chemical Co. (St. Louis, MO). The polyamine analogue DENSPM was kindly supplied by Warner Lambert Parke Davis (Ann Arbor, MI). MALME-3M containing wild-type p53 and SK-MEL-28 containing mutated p53 human melanoma (26) were purchased from the American Type Culture Collection (Bethesda, MD).

Cell Culture. MALME-3M and SK-MEL-28 human melanoma cells were maintained as monolayer cultures growing in RPMI 1640 containing 10% Nu-Serum (Collaborative Research Products, Bedford, MA) and 1 mM of aminoguanidine as an inhibitor of serum polyamine oxidation. Under these conditions, both cell lines displayed similar doubling times of 40–45 h. Cells were seeded 24 h before treatment, and the time course for growth inhibition was assessed during treatment with 5 mM of DFMO, 10 μM of MDL-73811, or 10 μM of polyamine alone or in various combinations. For cell cycle and protein prevention studies, inhibitors plus 10 μM of Spd were all added at 0 h, and cells were assayed at day 3. Longer exposures (*i.e.*, >6 days) required reseeding of cultures at day 3. For growth recovery studies after 8 days of exposure to inhibitors, cultures were washed three times with sterile PBS and placed in FM. Cell number was determined electronically using a Model ZM Coulter Counter (Coulter Electronics, Hialeah, FL). For time course experiments, treatments were staggered to process the untreated and treated samples at similar cell densities (*i.e.*, mid-log growth). To determine plating efficiency, cells were grown in the presence or absence of inhibitors for 8 days, trypsinized, counted, and resuspended in fresh medium containing 20% serum and plated into six-well plates at 500, 100, and 2000 cells/well. After 2 weeks, colonies were stained with methylene blue and counted. Only colonies containing >20 cells were scored as positive.

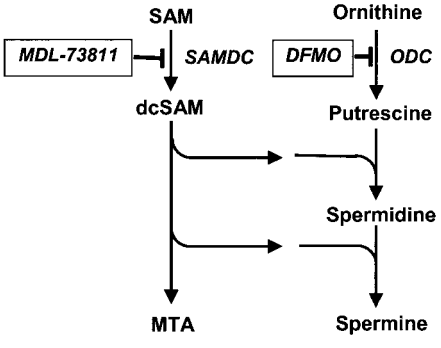

Fig. 1. Diagram of polyamine biosynthetic pathway showing the target enzymes of the polyamine biosynthetic inhibitors DFMO and MDL-73811. By inhibiting ODC, DFMO depletes Put and Spd pools, whereas it only modestly affects Spm pools. By inhibiting SAMDC, MDL-73811 depletes Spd and Spm, whereas it markedly increases Put. The inhibitor combination lowers all three polyamine pools until cells stop growing and the pools are no longer diluted by cell division.

Polyamine Pools. Intracellular polyamines were extracted from cell pellets with 0.6 N perchloric acid at a ratio of 2×10^7 cells/ml, dansylated, and measured by reverse phase high-performance liquid chromatography as described previously (22) with the following modifications. Dansylated samples (50 μl) were injected onto a 250 mm × 3.2 mm ID Econosil C18 column (5 μm particle size; Alltech, Deerfield, IL) with a column temperature of 50°C and eluted by a two solvent gradient using a Waters 616 LC system (Waters Assoc., Milford, MA) and a Waters WISP 710B autosampler. Solvent A contained 55% of 10 mM ammonium phosphate/45% acetonitrile (pH 4.4). Solvent B contained 100% acetonitrile. At 0.9 ml/min, the gradient began at 100% solvent A and progressed linearly to 82% solvent B over 30 min with a 15 min hold. Compounds were detected using a McPherson FL-750 BX fluorescence detector (Acton Research Corp., Acton, MA) with an excitation wavelength of 360 nm and an emission cutoff filter of 500 nm. The data were collected and analyzed using Waters Millennium 32 chromatography software version 3.05 (Waters Assoc.).

Flow Cytometry. Cell samples were stained with propidium iodide using a procedure described by Krishan (27) and subjected to flow cytometric analysis using a FACScan flow cytometry unit (Becton Dickinson, San Jose, CA) available at the Roswell Park Cancer Institute Core facility under the direction of Dr. Carleton Stewart. Forward *versus* side scatter plots were used to determine changes in cell size and granularity.

Apoptosis. Cells were stained with annexin V to detect phosphatidylserine using a commercial apoptosis kit (R & D Systems, Minneapolis, MN) and analyzed by flow cytometry. Additional confirmation of apoptosis was carried out by quantitative morphological analysis of attached and detached cell populations stained with H&E as described previously (21).

BrdUrd Incorporation. Cells were treated for 8 days with inhibitors and reseeded into six-well plates in the presence of inhibitors or FM for an additional 2 days with exposure to 2.5 μM of BrdUrd (stock solution is 1 mM in PBS and stored at −20°C) for DNA labeling. Cell pellets were resuspended in ice-cold 70% ethanol and stored at −20°C until analysis. Detection of incorporated BrdUrd has been described in detail elsewhere (28). In short, the denatured DNA is exposed to primary anti-BrdUrd (MO74401; Dako Corp., Carpinteria, CA) and a FITC-conjugated secondary (FO31302; Dako Corp.). The DNA was also stained with propidium iodide and evaluated by flow analysis. The red (DNA) and green (BrdUrd) fluorescent signals were stored as list data files for analysis by the Winlist software program (Verity Software House Inc., Topsham, ME). After minimizing the contribution of nuclear doublets by electronic threshold settings (29) the nuclei were displayed in DNA *versus* BrdUrd cytograms to determine the percentage of BrdUrd-labeled cells.

Western Blot Analysis. Antibodies used for detecting specific cell cycle regulatory proteins by standard Western techniques were obtained commercially as follows. Mouse monoclonal p53 (DO-1, sc-126), goat polyclonal p18 (N-20, sc-865), Kip2/p57 (H-17, sc-1038), and tyrosinase (C-19, sc-7833) were obtained from Santa Cruz Biotechnology, Inc. (Santa Cruz, CA); mouse monoclonal Rb (14001A), p21 (65961A), and p16 (13251A) from PharMingen (San Diego, CA); mouse monoclonal p27 (K25020), from Transduction Labs (Lexington, KY); mouse monoclonal mdm-2 (OP46), cyclin D1 (Ab-1, CC04), and cyclin E (Ab-1, CC05) from Calbiochem-Novabiochem Corporation (San Diego, CA); and mouse monoclonal β-actin (A-5316) from Sigma Chemical Co. Cell cultures were carefully maintained in a constant semiconfluent and logarithmically growing state throughout each experiment. Multiple controls seeded at varying densities yielded similar protein signals (data not shown).

***β*-Gal Staining.** SA-β-gal activity was determined as described previously (30) with some modifications. Briefly, cells were grown on coverslips and treated with 5 mM of DFMO plus 10 μM of MDL-73811 for 4, 6, 8, 10, and 14 days. Cells were fixed in 0.25% glutaraldehyde in PBS for 15 min, washed three times with PBS, and stained using fresh buffer [1 mg of 5-bromo-4-chloro-3-indolyl-β-D-galactoside/ml (stock 40 mg/ml DMSO)/5 mM potassium ferrocyanide/5 mM potassium ferricyanide/2 mM $MgCl_2$/PBS] at 37°C (in a

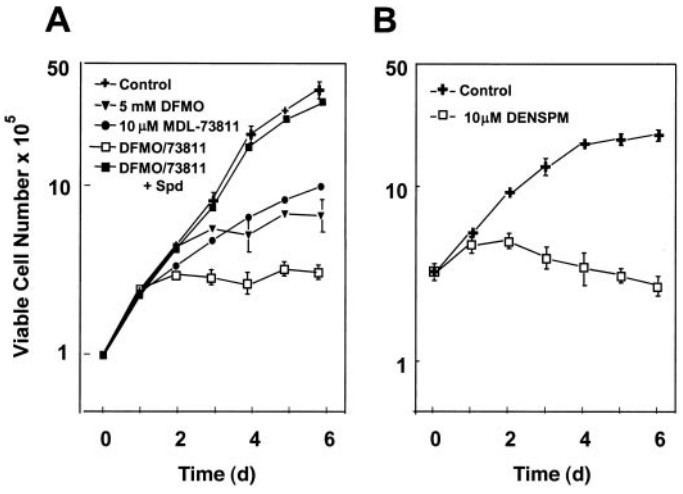

Fig. 2. A comparison of time-dependent effects of 5 mM DFMO and 10 μM MDL-73811 used singly and in combination (*A*) and 10 μM DENSPM (*B*) on MALME-3M cell growth. Note that cells treated with both inhibitors are fully growth inhibited from day 2 onwards, whereas individual inhibitors only slow the growth rate. Exogenous Spd (10 μM) completely prevented antiproliferative effects of inhibitors alone or in combination. The response to DENSPM is an immediate growth arrest followed by a gradual cell loss attributable to apoptosis. Data represent the average cell number from at least three separate determinations; *bars*, ± SD.

CO_2 incubator) for 8–14 h. Under these conditions, the pH of the staining buffer remained at ~6.5. β-Gal will cleave 5-bromo-4-chloro-3-indolyl-β-D-galactoside forming a local blue precipitate in a pH range of 6–7 (lysosomal β-gal activity is optimally active at pH 4). The coverslips were mounted and >500 cells were scored to determine percentage of blue-stained cells. Light micrographs were taken using a RTSlider Spot digital camera equipped with the Spot Advanced Software, Version 3.1 (Diagnostics Instruments, Inc., Sterling Heights, MI) linked to a phase contrast Nikon Optiphot microscope (Nikon Corporation, Tokyo, Japan).

Hoechst Staining. Cells were grown on coverslips as described above and at the end of treatment exposed for 15 min to 0.5 μM of Hoechst dye added directly to the culture medium. The coverslips were fixed in 70% methanol and mounted on slides. Using an Olympus BX40 epifluorescence microscope (Olympus America, Inc., Melville, NY) equipped with a universal reflected light fluorescence vertical illuminator and attached to an RT-SPOT color digital camera (Diagnostic Instruments, Inc.), at least 200 cells/condition were captured with the ×60 objective by both phase contrast and fluorescent images (wide UV cube with an exitation filter at 360–370 nm and barrier filter at 420–460 nm) for quantitation.

RT-PCR Analysis. RNA samples were isolated from control and treated cell pellets using a Rneasy mini kit (74104; Qiagen Inc., Valencia, CA). cDNA synthesis and RT-PCR analysis were carried out essentially as described (31) using β-actin as an internal standard for cDNA normalization. The expression patterns were determined on samples obtained from two separate experiments.

RESULTS

Cell Growth, Polyamine Pools, and Cell Cycle Distribution. Logarithmically growing human melanoma MALME-3M cells were exposed to 5 mM of DFMO, 10 μM of MDL-73811, or the combination of both inhibitors for up to 6 days (Fig. 2*A*). Whereas individual inhibitors caused a modest slowing of cell growth after 2–3 days, the inhibitor combination produced a distinct and near-total cessation of cell growth at 2 days. Inhibitor effects on polyamine pools (Table 1) followed trends seen in other cell types (32). Inhibition of ODC with DFMO depleted Put and Spd pools and decreased Spm pools slightly. Inhibition of SAMDC with MDL-73811 increased Put enormously and reduced Spd and Spm pools. Combined inhibition of both enzymes depleted Spd and Spm pools and prevented the increase in Put pools seen with MDL-73811. Maximum polyamine pool depletion occurred at 3 days of treatment after which polyamine pools remained relatively unchanged.

Inhibitor effects on cell cycle kinetics are shown in Table 1. After 3 days of treatment, the individual inhibitors, DFMO or MDL-73811, produced only minor shifts in cell cycle distribution, most notably represented as a subtle increase in G_1 cells with a slight reduction in S phase cells. Longer treatment failed to induce a more defined cell cycle arrest (data not shown). By comparison, treatment with the combination of inhibitors resulted in a distinct and progressive accumulation of cells in G_1 and reduction in S phase cells, a profile characteristic of G_1 arrest. As with polyamine pools, this population shift progressed steadily during the first 3 days after which it remained relatively constant from days 3 to 6 with the majority of cells (approximately 85–90%) in G_1 and only a small portion (<10%) in G_2-M. When these same data are expressed graphically (Fig. 3), the earliest significant reduction in S phase cells relative to untreated cells (day 0) occurred at 1.5 days of treatment. This shift correlated closely with a significant decline in Spd and Spm pools that also took place at this same time (Fig. 3). Cotreatment with inhibitors plus 10 μM Spd maintained Spd pools and prevented G_1 arrest (Table 1), as well as growth inhibition (Fig. 2*A*), thus indicating a causal relationship with polyamine pool depletion. A similar prevention of growth inhibition could be achieved using either Spd or Spm (data not shown).

Changes in Cell Cycle Regulatory Proteins: Strong and Rapid Induction of p21. To investigate the mechanism of G_1 arrest induced by polyamine depletion, we have analyzed changes in p53, p21, Rb, and several other proteins that regulate G_1-S transition in cells treated with the combination of two inhibitors. Fig. 4*A* shows the results of immunoblotting assays, which are quantitated for several G_1-associated proteins in Fig. 4*B*. The earliest and the strongest change among all of the tested proteins was observed with p21, which increased 4-fold by 1.5 days and >10-fold by day 6 of treatment. cdk inhibition by p21 is known to cause dephosphorylation of Rb, and we have

Table 1 *Effects of polyamine inhibitors on cell cycle phase distribution and polyamine pools in MALME-3M human melanoma cells*

Treatment[a]	Time (d)	Growth (% control)	Cell cycle (% Total cells)			Polyamine pools (pmol/10^6 cells)		
			G_1	S	G_2/M	Put	Spd	Spm
Control	3	100	65	21	14	1275	3375	3150
5 mM DFMO	3	83	72	17	11	<20	225	2790
10 μM MDL-73811	3	72	74	15	11	8890	1140	860
DFMO + MDL-73811	1	97	71	17	13	1280	2965	2630
	1.5	75	73	10	16	835	2110	2015
	2	65	81	8	11	890	1850	1530
	3	40	86	5	9	685	1655	1300
	4	22	89	3	7	625	1650	1295
	6	22	88	4	8	480	2000	1280
DFMO + MDL-73811 + 10 μM Spd	3	92	72	18	11	320	5665	430

[a] Data represent mean values from at least three separate experiments with SD values <15% (see Figure 3).

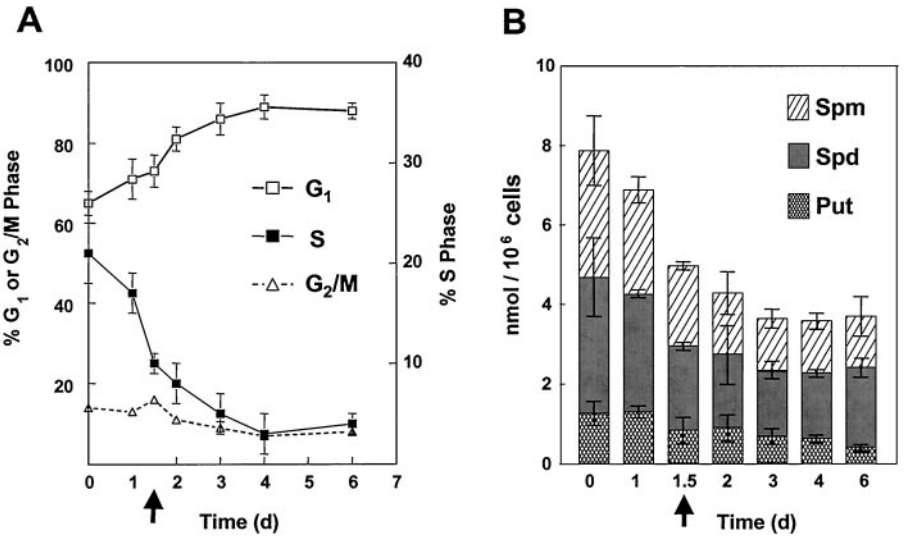

Fig. 3. Time-dependent effects of treatment with 5 mM DFMO plus 10 μM MDL-73811 on cell cycle distribution and polyamine pools. Cell cycle data in *A* represent relative percentage of total cells in G_1 and G_2-M (*left axis*) or S (*right axis*) phases of the cell cycle. Note that G_1 arrest becomes obvious at day 1.5 (*arrow*) as indicated by the concomitant increase in cells in G_1 and a decrease in those in S. *Stacked bars* in *B* represent the pools of Put, Spd, and Spm. The first significant decrease in total pool size occurred at day 1.5 (*arrow*). These data derive from at least five separate determinations; *bars*, ± SD.

observed a decrease in Rb phosphorylation starting on day 2 with a visible reduction in the hyperphosphorylated form (upper major band, ppRb) by 3 days. Rb dephosphorylation was followed by a decrease in the total cellular level of Rb (day 6); a similar decrease was observed previously on p21 induction in HT1080 fibrosarcoma cells (31) and in normal fibroblasts undergoing replicative senescence (33). The relationship of these protein changes to polyamine pool depletion was confirmed by the finding that at 10 μM exogenous Spd prevented induction of p21, maintained phosphorylation of Rb (Fig. 5), and allowed cells to continue cycling (Table 1).

In addition to rapid changes in p21, we have found a 2–3-fold increase in another cdk inhibitor, p27, after 4 days of treatment when cycle arrest was already established (Fig. 4). Three other cdk inhibitors, p16, $p18^{Ink4C}$, and $p57^{Kip2}$, were undetectable by immunoblotting in treated or untreated cells. The lack of p16 in MALME-3M melanoma cells (22) is consistent with a mutation or deletion of the *INK4a* locus (34), a common genetic change among melanoma tumors. Cyclin D1 and E levels were not significantly affected by the inhibitors, remaining similar to untreated cells during the entire treatment period. Taken together, these results indicate that strong and rapid p21 induction is responsible at least in part for the inhibitor-induced G_1 arrest.

Levels of p53 protein remained relatively unchanged until day 3 when they increased nearly 2-fold and then to 4-fold by day 6 (Fig. 4). Because p21 was induced as early as 1–1.5 days, this result suggested that the initial p21 induction in polyamine-depleted cells was independent of p53. In support of this interpretation, the levels of mdm-2, another protein that is transcriptionally activated by p53 (35), did not rise significantly until day 3 (Fig. 4). Attempts to test the role of p53 in p21 induction by transiently transfecting a dominant-negative p53 mutant into MALME-3M cells were confounded by unacceptably low transfection efficiencies in this cell line. As an alternative approach, p21 induction by polyamine depletion was examined in SK-MEL-28 melanoma cells. The latter are similar to MALME-3M cells in both growth and polyamine metabolism (22) but differ by having a mutation in the DNA-binding region of p53 protein that renders it inactive (26). The polyamine inhibitor combination caused SK-MEL-28 cells to undergo growth inhibition and cell cycle arrest similar to that seen in MALME-3M cells (data not shown). Immunoblotting analysis (Fig. 6) revealed that despite the absence of a functional p53, p21 was

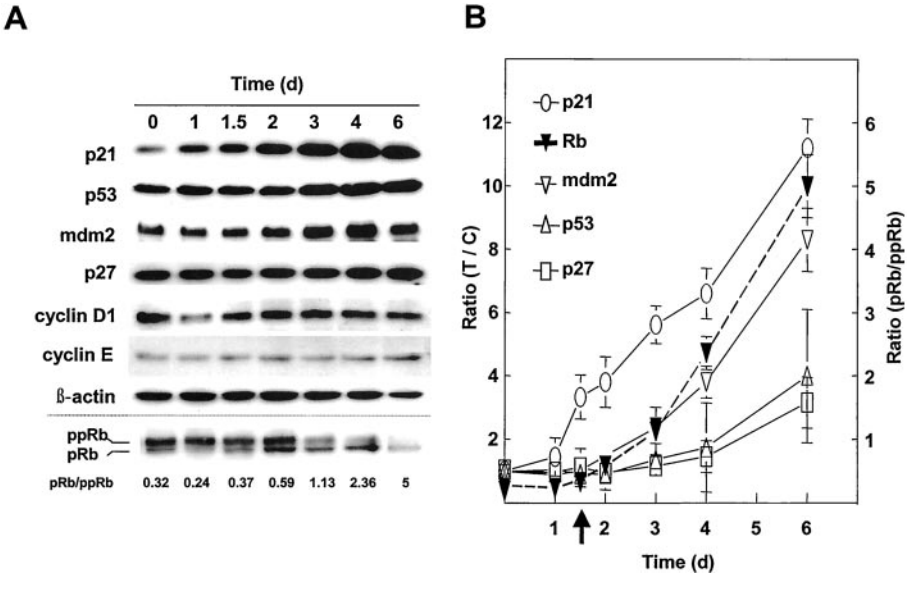

Fig. 4. Western blot analysis (*A*) of time-dependent effects on cell cycle regulatory proteins p21, p53, mdm-2, p27, cyclin D1, cyclin E, and Rb in MALME-3M cells treated from 0 to 6 days with 5 mM DFMO plus 10 μM MDL-73811. Bands for Rb are designated as ppRb, hyperphosphorylated protein (*top band*) and pRb, hypophosphorylated protein (*bottom band*). The ratios of pRb:ppRb are values taken from *B*. *B*, relative changes in cell cycle regulatory protein expression based on quantitation of Western blots. Proteins were scanned and fold protein changes (treated/control) normalized relative to β-actin protein for p21, p53, mdm-2, and p27 (*left axis*). The ratio of pRb:ppRb (*right axis*) was calculated relative to 0 h. *Arrow*, obvious induction of p21 at 1.5 days. These data are representative of at least three separate determinations; *bars*, ± SD.

induced 2-fold at 2 days and increased to 15-fold by 4 days. In contrast to MALME-3M, cdk inhibitor p16 was expressed in SK-MEL-28 cells (34), but it increased by only 1.5-fold after 6 days. The G_1 arrest at ~2 days correlated with hypophosphorylation of Rb, which continued until 6 days when the hypophosphorylated form (pRb) became predominant. Therefore, polyamine depletion induces p21 expression and cell cycle arrest in these p53-deficient tumor cells, indicating that p21 induction is at least partially mediated by p53-independent mechanisms.

Effects of p21 Induction on Gene Expression. We have found previously that p21 expression from an inducible promoter in HT1080 fibrosarcoma cells has pleiotropic effects on cellular gene expression (31). These included inhibition of multiple genes involved in cell cycle progression and induction of genes associated with cell senescence, paracrine growth stimulation, and age-related diseases. We have now asked whether p21 induction resulting from polyamine depletion in MALME-3M would have similar effects on gene expression. For this analysis, RNA samples were isolated from cells grown in the presence and absence of inhibitors for up to 10 days. These samples were analyzed by RT-PCR for changes in the expression of p21 and of 20 other genes that were shown previously to be down- or up-regulated by p21 induction in HT1080 cells (31).

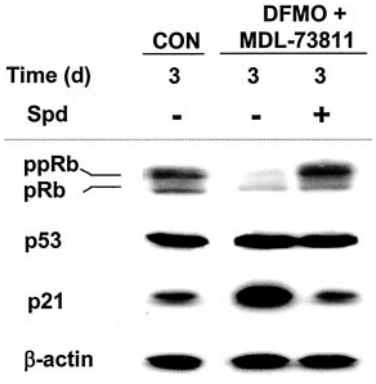

Fig. 5. Prevention of p21 induction and the shift in Rb phosphorylation by 10 μM Spd cotreatment with 5 mM DFMO plus 10 μM MDL-73811 for 3 days. Cells treated with 10 μM Spd alone appeared as control. Data are representative of two separate experiments.

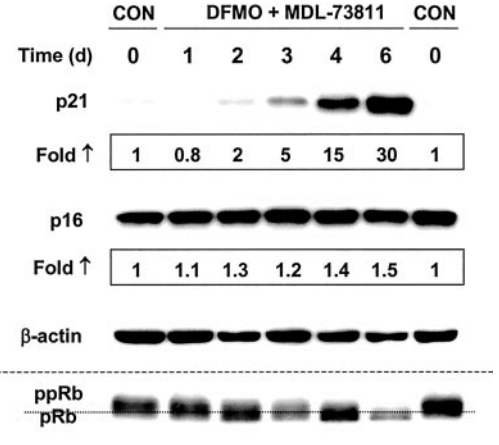

Fig. 6. Western analysis of p21, p16, and Rb proteins in SK-MEL-28 human melanoma cells (mutated p53) treated with 5 mM DFMO plus 10 μM MDL-73811 for 1 to 6 days. Fold-induction data (treated/control normalized relative to β-actin protein) are representative of three separate determinations. Control samples (day 0) were loaded in the *first* and *last lanes* for orientation, especially for Rb. ----, drawn through the Rb protein to distinguish the upper (*ppRb*) from the lower (*pRb*) bands.

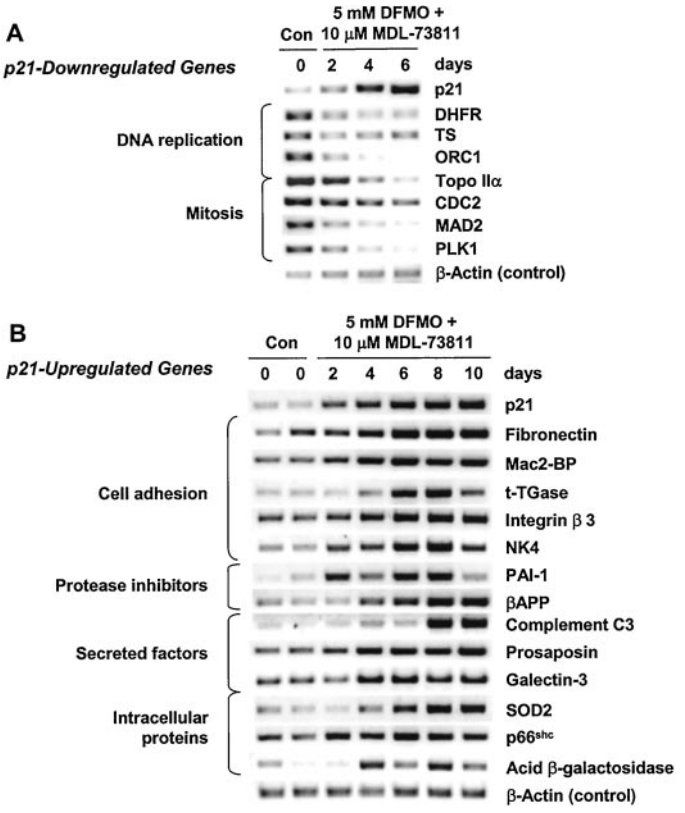

Fig. 7. RT-PCR analysis of samples derived from MALME-3M cells grown in the absence of inhibitors (0 day points) or in the presence of inhibitors from (*A*) 2 to 6 days to measure expression of p21-inhibited genes or from (*B*) 2 to 10 days to measure expression of p21-induced genes. Expression of p21 was determined on both sample sets and β-actin was included as a normalization standard. These data are representative of similar results obtained from two separate experiments.

The results of this analysis are shown in Fig. 7. In agreement with the results of protein analysis in Fig. 4, we observed a major rise in p21 RNA levels at day 2 (the earliest point of RNA analysis in treated cells) followed by a steady increase through day 10 of treatment (Fig. 7, *A* and *B*). p21 induction was accompanied by down-regulation of seven of seven tested genes shown previously to be inhibited by p21 induction (Fig. 7*A*). These include: (*a*) replication-associated genes *DHFR* and *TS;* (*b*) *origin recognition complex* and *Topo II*α, involved in DNA and chromosome segregation; and (*c*) mitosis-associated genes *CDC2* (mitosis-initiating kinase), *PLK1* (a regulator of multiple steps of mitosis), and *MAD2* (spindle checkpoint control; Fig. 7*A*).

Polyamine depletion also led to up-regulation of 13 of 14 tested p21-inducible genes (the only exception was *serum amyloid A*, which was undetectable in all of the samples). These genes encode proteins involved in cell adhesion such as fibronectin, Mac2-BP, t-TGase, integrin-β3, and NK4. Other genes encode secreted proteins such as plasminogen activator inhibitor 1 (PAI-1) and complement C3 and antiapoptotic factors prosaposin and galectin-3. Polyamine depletion also induced Alzheimer's βAPP; stress response proteins SOD2 and p66Shc; and lysosomal enzyme acid β-gal (Fig. 7*B*). Taken together, the results of RT-PCR analysis demonstrate that polyamine depletion in melanoma cells not only induces p21 but, if sustained, also reproduces the complex pattern of changes in gene expression observed previously on p21 induction in fibrosarcoma cells (31).

p21 Induction Is Associated with Phenotypic Features of Cell Senescence. p21 expression in different cell lines has been shown to produce the senescent phenotype (36–38), and several genes induced by polyamine depletion in MALME-3M cells have been described as markers of cell senescence. These include *βAPP*, *PAI-1*, *fibronectin*,

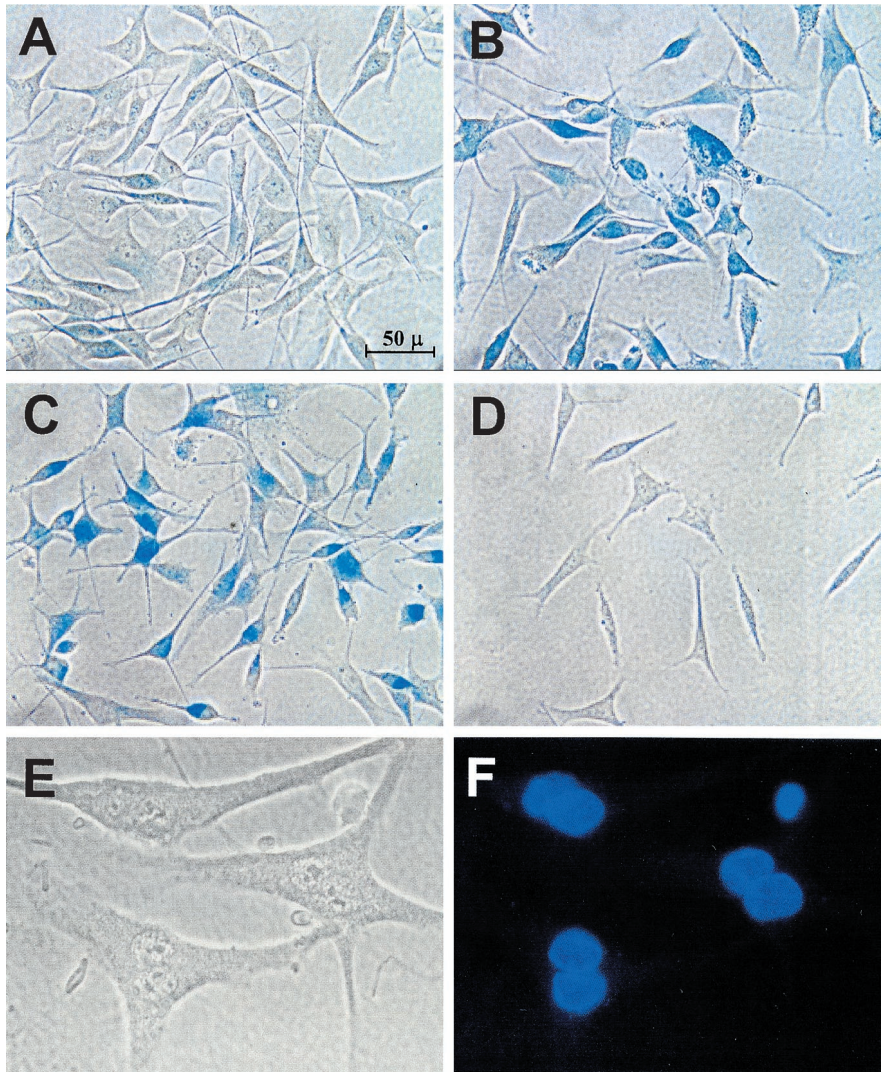

Fig. 8. Representative photomicrographs of MALME-3M cells grown in the absence (*A*) or presence (*B*) of 5 mM DFMO plus 10 μM MDL-73811 for 8 days and stained for SA-β-Gal activity at pH 6.5. *C*, staining for MALME-3M cells treated with inhibitors, washed, and placed in fresh FM from day 8 to 12. *D*, lack of staining in MALME-3M cells after a 6-day exposure to 10 μM DENSPM. *E* and *F*, binucleated cells by phase contrast and fluorescent microscopy, respectively, from cultures treated with the inhibitor combination for 8 days (stained with Hoechst dye). Cell size is relative to the 50-μm *bar*.

integrin β3, and acid *β-gal* (30). Thus, we investigated whether polyamine depletion also induces phenotypic features of cell senescence (39) such as increased cell size and granularity and staining for the SA-β-Gal marker of senescence. Untreated MALME-3M cells (Fig. 8*A*) and cells treated with inhibitors (Fig. 8*B*) were stained for SA-β-Gal at various times over a 14-day treatment period. The percentage of SA-β-gal positive cells increased steadily with time starting at day 6 and reaching a maximum of ~60% by day 10 (Fig. 9). SA-β-Gal expression was not apparent in MALME-3M cells treated for 6 days with the polyamine analogue DENSPM (Fig. 8*D*), which, as mentioned below and elsewhere (21, 22), induces apoptosis.

Changes in cell size and granularity were investigated by flow cytometric assays through examination of the forward *versus* side scatter plots. The profiles (Fig. 10) show that after 8 and 13 days of treatment, the entire cell population was slightly larger and considerably more granular. Although clearly detectable by flow cytometry, changes in cell size and granularity of MALME-3M cells at the microscopic level were not as obvious as has been reported in normal melanocytes undergoing replicative senescence (40). The latter study also reported that some of the senescent (but not differentiating) melanocytes develop multiple nuclei (40). After prolonged treatment with inhibitors, Hoechst-stained MALME-3M cells showed an increase in binucleated cells (Fig. 8, *E* and *F*), which were <5% without treatment. After 15 days of treatment, 23% of the cells were binucle-

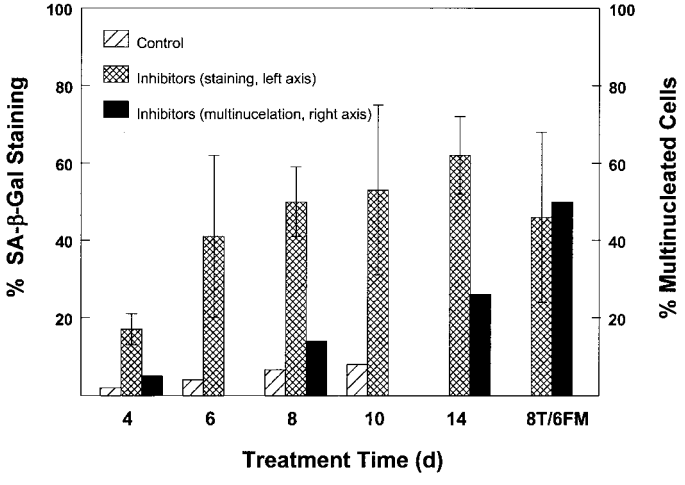

Fig. 9. Quantitation of the effects of polyamine depletion on the expression of SA-β-Gal (*left axis*) and the appearance of multinucleated cells (*right axis*). MALME-3M cells were grown on coverslips and stained for SA-β-Gal activity after 4, 6, 8, 10, and 14 days in the absence (▨) or presence (▩) of 5 mM DFMO plus 10 μM MDL-73811 (*Inhibitors*). Data are based on three separate experiments with at least 500 cells scored per time point. The percentage of multinucleated cells (■, *right axis*) visible after Hoechst staining was determined after 4, 8, and 14 days of inhibitor treatment. Phase and fluorescent images were taken of at least 200 cells/condition. The *last two bars* represent data obtained on cells treated for 8 days, washed, and placed in fresh FM for an additional 6 days (*8T/6FM*); *bars*, ± SD.

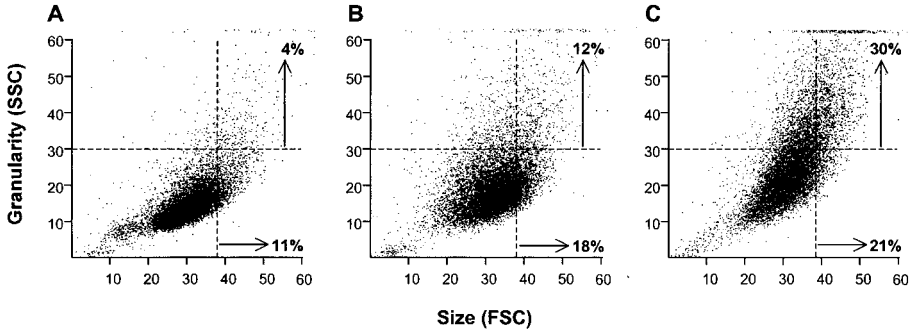

Fig. 10. Cells were grown in the absence or presence of inhibitors to determine the effects of polyamine depletion on size and granularity. Forward (*FSC*) and side (*SSC*) scatter images were obtained from samples stained with propidium iodide and analyzed by flow cytometry. After 10,000 cell events were collected, cells treated for 8 days (*B*) showed a more diffuse pattern than control (*A*), and by day 13 (*C*) there was a significant increase in both size and granularity. *Dashed lines* were included as arbitrary limits to show that by conservative estimates there was a 21% increase in size and 30% increase in granularity; however, there was a noticeable shift in the entire cell population.

ated, and another 3% had three or more nuclei. Taken together, the morphological data support the emergence of the senescent phenotype in polyamine-depleted cells.

Long-Term Effects of Polyamine Depletion. The senescent phenotype was shown previously to distinguish drug-treated tumor cells that have lost their proliferative capacity from the cells that recovered and resumed proliferation after drug exposure (36, 41). Therefore, we have investigated whether the senescent phenotype of polyamine-depleted MALME-3M cells was also associated with a long-term loss of their proliferative capacity. We have found that prolonged growth arrest of polyamine-depleted MALME-3M cells could not be reversed when cultures were washed free of inhibitors in fresh medium (Fig. 11). This was additionally confirmed by examining the ability of these cells to incorporate BrdUrd, a sensitive indicator of DNA synthesis. After 8 days of inhibitor treatment, cells were washed and placed in BrdUrd-containing FM for 2 additional days. After the initial treatment period, 90% of control cells incorporated BrdUrd as compared with only ~15% of inhibitor treated cells (Fig. 11, *inset*). Inhibitor removal and replacement with fresh medium increased this percentage only slightly. Cells treated with inhibitors for 8 days were also subjected to a colony-forming assay to additionally evaluate their ability to divide. Because MALME-3M growth is very density dependent, plating efficiency of these cells is only 16 ± 3% in such assays. This was reduced to 0.6 ± 0.2% for inhibitor-treated cells. This 27-fold decrease in colony formation indicates that polyamine depletion results in irreversible loss of proliferative capacity.

The irreversible inhibition of inhibitor-treated MALME-3M cells was not attributable to apoptosis. There was no indication of apoptosis by either the appearance of a sub-G_1 peak or by annexin V staining, even after treatments as long as 12 days. However, the viable cell number decreased by day 18 of treatment as the treated cells began to detach and stain positively for propidium iodide and negatively for annexin V, indicating nonapoptotic cell death (data not shown). As a positive control, apoptosis was readily detectable by this assay in DENSPM-treated cells, in agreement with previous results (21). We found 50% of the cells stained positive for annexin V after DENSPM treatment for 4 days (data not shown). These data coincide with the gradual decrease in viable cell number during DENSPM treatment shown in Fig. 2*B*.

In contrast to the lack of apoptosis, two morphological observations are likely to account for the proliferative failure of polyamine-depleted MALME-3M cells. The first observation is the maintenance of a high percentage of SA-β-gal-positive cells for as long as 4 days after release from the inhibitors (Figs. 8*C* and 9), indicating maintenance of the senescent phenotype. The second observation was an increase to 50% in the fraction of cells with two or more nuclei, observed when the cells were placed in fresh medium from 8 to 14 days (Fig. 9). This process of micronucleation is indicative of mitotic catastrophe, which is routinely observed on exposure to different chemotherapeutic drugs (41) or after release from p21-induced growth arrest (42). These observations suggest that polyamine-depleted MALME-3M cells lose their proliferative capacity through senescence-like terminal growth arrest and mitotic catastrophe.

Finally, tyrosinase, the enzyme responsible for melanin production (43), was measured to test the possibility that these inhibitor-treated cells were progressing toward terminal differentiation. Tyrosinase protein levels remained unchanged during polyamine depletion until 8 days of treatment when they increased 2–3-fold (data not shown). This suggests that, if invoked by polyamine depletion, differentiation is a late-stage event that follows those associated with the p21-induced senescent-like phenotype.

DISCUSSION

We have analyzed the cell cycle responses and cellular outcomes to polyamine depletion on MALME-3M melanoma cells. The observed effects relate exclusively and directly to the depletion of polyamine pools, because: (*a*) the inhibitors used in this study are mechanism-based and highly specific for polyamine biosynthetic enzymes; and (*b*) the effects of the inhibitors are all fully preventable with exogenous polyamines. Our analysis indicates that polyamine pool deple-

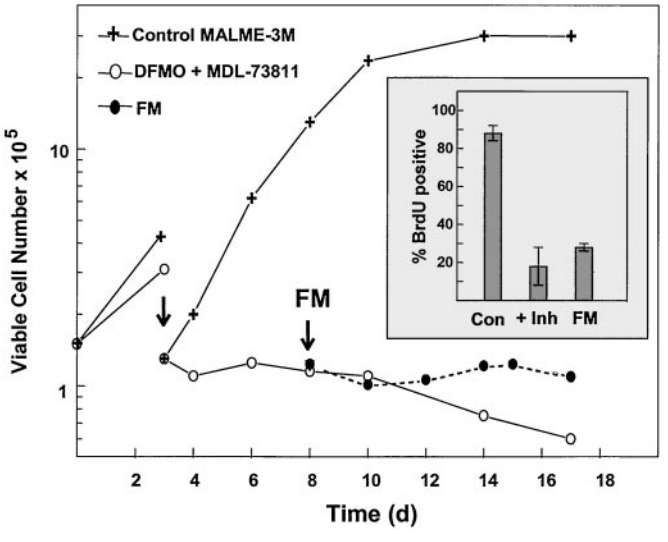

Fig. 11. Growth of MALME-3M cells maintained in 5 mM DFMO plus 10 μM MDL-73811 for 17 days. At day 3 (*arrow*), control and treated cells were reseeded to similar cell densities maintaining treatment conditions. At day 8, treatment was either continued or halted by placing cells in fresh medium (*FM, broken line at arrow*) for an additional 9 days. *Inset*, determination of the DNA synthetic rate by BrdUrd incorporation. Cells treated for 8 days with 5 mM DFMO plus 10 μM MDL-73811 were either retreated for 2 additional days with inhibitors (*+ Inh*) or washed and placed in fresh FM both in the presence of 2.5 μM BrdUrd. Cell samples were prepared as described in "Materials and Methods," and the percentage of BrdUrd incorporation was determined on treated cells and untreated logarithmically growing cells (*Con*). The 2-day labeling period, equivalent to one doubling time for MALME-3M cells, allowed ~90% of the control cells to incorporate BrdUrd.

tion causes a G_1 arrest that is temporally related to strong induction of cdk inhibitor p21; no other tested cdk inhibitors showed comparable induction under these conditions. p21 induction in polyamine-depleted cells is followed by a complex set of molecular and cellular changes. These changes parallel in minute detail the effects of p21 expression from an inducible promoter, described previously in a fibrosarcoma cell line (31, 36, 42). These effects of p21 can account for the observed G_1 arrest, development of phenotypic features of cell senescence, and loss of cellular proliferative capacity on release from polyamine inhibitors.

The initial p21 induction by polyamine depletion is mediated in part by p53-independent mechanisms. This conclusion is indicated by the following results. Firstly, p53 levels are increased on polyamine depletion in MALME-3M cells (indicative of p53 protein stabilization), but this increase occurs much later than p21 induction. Transcriptional stimulation by p53 could conceivably increase before protein stabilization, *e.g.*, through intracellular redistribution of p53. However, this does not seem to be the case in our cells, because mdm-2, another target of transcriptional activation by p53, is induced only after p53 stabilization. Secondly, polyamine depletion strongly induces p21 not only in MALME-3M, but also in SK-MEL-28 cells, which express a p53 mutant incapable of transcriptional activation (26). The mechanism of p53-independent p21 induction in polyamine-depleted cells remains to be investigated. A candidate mediator of this effect is c-*myc*, a negative regulator of p21 transcription (44) and a positive regulator of ODC (6–8), which was shown to be down-regulated by polyamine depletion in COLO320 carcinoma cells (45). Whereas the initial p21 induction does not appear to be solely dependent on p53, subsequent increases in p53 stabilization correlated with the intensification of p21 expression suggesting a role for the protein in sustaining the p21 response.

In contrast to the inhibitor combination, the polyamine analogue DENSPM rapidly and concurrently induces both p53 and p21 in MALME-3M cells. However, DENSPM does not induce p21 in p53-deficient SK-MEL-28 cells (22). Therefore, analogue-induced p21 expression appears to be p53-dependent. Analogues also induce cell cycle arrest followed by apoptosis (22), while as shown here, the inhibitor combination causes predominantly cytostatic growth arrest with no apoptosis. These differences may be because analogues bring about rapid and near-total polyamine pool depletion whereas inhibitors reduce pools by only ~50% because of the fact that cessation of growth limits additional pool dilution. In addition, analogues induce polyamine catabolism, whereas inhibitors do not. Therefore, it is possible that limited pool reduction ($\leq$50%) may be sufficient to trigger a p53-independent response, whereas additional ($\geq$50%) or sustained reduction may recruit p53. It is also possible that analogue-induced apoptosis is attributable to the rapidity and extent of polyamine pool depletion or, alternatively, to some direct effect of the analogue.

Induction of p21 in polyamine-depleted MALME-3M cells was followed by molecular changes that are known to account for cell cycle arrest. One of the molecular changes responsible for cell cycle arrest seen is dephosphorylation of pRb, apparently as a result of p21-mediated inhibition of cdk2 and cdk4/6 (46). The hypophosphorylated pRb acts as a growth inhibitor, partly by sequestering and inhibiting E2F transcription factors, which act as positive regulators of many genes involved in cell proliferation. Indeed, all seven of the tested proliferation-related genes (shown previously to be inhibited by p21) were also inhibited in polyamine-depleted cells. These include E2F-regulated genes such as *DHFR* and *TS*, as well as genes that do not contain E2F sites in their promoters (such as *Topo IIα*). The role of Rb and other pocket proteins in p21-mediated inhibition of gene expression is a subject of ongoing investigation.

Polyamine depletion has also resulted in phenotypic changes associated with cell senescence such as increased cell size and granularity, flattened morphology, and expression of the senescence marker SA-β-gal. The senescent phenotype has been shown to result from p21 induction in different tumor cell lines (41). At least some aspects of this phenotype are associated with the functions of p21-inducible genes, 13 of which (of 14 tested) are shown here to be up-regulated by polyamine depletion in MALME-3M cells. Although p21-inducible genes are not functionally involved in cell growth arrest, they play a role in various phenotypic changes associated with cell senescence and organism aging. For example, fibronectin, Mac2-BP, and t-TGase contribute to increased cell adhesion and flattened cell shape, and acid β-gal is likely to be responsible for the SA-β-gal activity of senescent cells (30). Notably, t-TGase, which uses polyamines as natural substrates, was shown previously to be induced at the mRNA level by polyamine depletion (47). Other induced genes encode secreted proteins that affect neighboring cells and tissues such as PAI-1 (48) and antiapoptotic factors prosaposin and galectin-3 (49, 50). Induction of secreted antiapoptotic factors as well as SOD2 that inhibits apoptosis by acting as a negative regulator of cytochrome C release from mitochondria (51) may account for the lack of detectable apoptosis in polyamine-depleted cells. p21-inducible genes have been associated not only with cell senescence but also with organism aging and age-related diseases (31). Of special note, $p66^{Shc}$, a mediator of oxidative stress, was shown to be a negative determinant of mammalian life span (52), whereas βAPP plays an essential role in Alzheimer's disease (53).

Prolonged polyamine depletion in MALME-3M cells results in >20-fold decrease in colony formation after release from the inhibitors. The effects of p21 induction can also explain this irreversible growth inhibition, which occurs in the absence of apoptosis. p21 expression from an inducible promoter in HT1080 cells results in both reversible and irreversible growth arrest, with the irreversible effects becoming predominant with increasing duration of p21 expression (42). The loss of clonogenicity after prolonged p21 expression was found to be a result of mitotic abnormalities during the first cell division after release from p21. This abnormal mitosis was associated with p21-mediated inhibition of mitosis-control genes (such as *MAD2* or *PLK1* in Fig. 7*A*) followed by their asynchronous resynthesis after the decay of p21. Cells that underwent abnormal mitosis then suffered terminal growth arrest accompanied by the senescent phenotype or died (42). Cell death on release from p21 was associated with the appearance of micronucleated cells, characteristic of mitotic catastrophe (41). The outcome of long-term polyamine depletion in MALME-3M cells was remarkably similar to the effects described above for p21 induction. After the removal of the inhibitors, most of the cells showed no detectable DNA replication (by the BrdUrd incorporation assay), with more than one-half of the cells maintaining the senescent phenotype (SA-β-gal positivity). On the other hand, the removal of inhibitors resulted in many cells developing micronuclei. Therefore, the observed combination of senescence-like terminal growth arrest and mitotic catastrophe explains the loss of clonogenic capacity after polyamine depletion as a long-term consequence of p21 induction.

ACKNOWLEDGMENTS

We thank Gregory Gan, Jing Fang, and Mei Shen for skilled technical assistance; and Slavoljub Vujcic, and Dr. Jennifer Black for helpful discussions.

REFERENCES

1. Mamont, P. S., Duchesne, M. C., Grove, J., and Bey, P. Anti-proliferative properties of DL-α-difluoromethyl ornithine in cultured cells. A consequence of the irreversible inhibition of ornithine decarboxylase. Biochem. Biophys. Res. Commun., *81:* 58–66, 1978.
2. McCann, P. P, and Pegg, A. E. Ornithine decarboxylase as an enzyme target for therapy. Pharmacol. Ther., *54:* 195–215, 1992.
3. Kahana, C., and Nathans, D. Isolation of cloned cDNA encoding mammalian ornithine decarboxylase. Proc. Natl. Acad. Sci. USA, *81:* 3645–3649, 1984.
4. Kaczmarek, L., Calabretta, B., Ferrari, S., and de Riel, J. K. Cell-cycle-dependent expression of human ornithine decarboxylase. J. Cell. Physiol., *132:* 545–551, 1987.
5. Fuller, D. J., Gerner, E. W., and Russell, D. H. Polyamine biosynthesis and accumulation during the G1 to S phase transition. J. Cell. Physiol., *93:* 81–88, 1977.
6. Bello-Fernandez, C., Packham, G., and Cleveland, J. L. The ornithine decarboxylase gene is a transcriptional target of c-Myc. Proc. Natl. Acad. Sci. USA, *90:* 7804–7808, 1993.
7. Wagner, A. J., Meyers, C., Laimins, L. A., and Hay, N. c-Myc induces the expression and activity of ornithine decarboxylase. Cell Growth Differ., *4:* 879–883, 1993.
8. Pena, A., Reddy, C. D., Wu, S., Hickok, N. J., Reddy, E. P., Yumet, G., Soprano, D. R., and Soprano, K. J. Regulation of human ornithine decarboxylase expression by the c-Myc. Max protein complex. J. Biol. Chem., *268:* 27277–27285, 1993.
9. Koza, R. A., and Herbst, E. J. Deficiencies in DNA replication and cell-cycle progression in polyamine-depleted HeLa cells. Biochem. J., *281:* 87–93, 1992.
10. Bergeron, C. J., Basu, H. S., Marton, L. J., Deen, D. F., Pellarin, M., and Feuerstein, B. G. Two polyamine analogs (BE-4–4-4 and BE-4–4-4–4) directly affect growth, survival, and cell cycle progression in two human brain tumor cell lines. Cancer Chemother. Pharmacol., *36:* 411–417, 1995.
11. Muller, R., Mumberg, D., and Lucibello, F. C. Signals and genes in the control of cell-cycle progression. Biochim. Biophys. Acta, *1155:* 151–179, 1993.
12. Packham, G., Porter, C. W., and Cleveland, J. L. c-Myc induces apoptosis and cell cycle progression by separable, yet overlapping, pathways. Oncogene, *13:* 461–469, 1996.
13. Anehus, S., Pohjanpelto, P., Baldetorp, B., Langstrom, E., and Heby, O. Polyamine starvation prolongs the S and G2 phases of polyamine-dependent (arginase-deficient) CHO cells. Mol. Cell. Biol., *4:* 915–922, 1984.
14. Fredlund, J. O., and Oredsson, S. M. Impairment of DNA replication within one cell cycle after seeding of cells in the presence of a polyamine-biosynthesis inhibitor. Eur. J. Biochem., *237:* 539–544, 1996.
15. Scorcioni, F., Corti, A., Davalli, P., Astancolle, S., and Bettuzzi, S. Manipulation of the expression of regulatory genes of polyamine metabolism results in specific alterations of the cell-cycle progression. Biochem. J., *354:* 217–223, 2001.
16. Pohjanpelto, P., Nordling, S., and Knuutila, S. Flow cytometric analysis of the cell cycle in polyamine-depleted cells. Cytometry, *16:* 331–338, 1994.
17. Porter, C. W., and Bergeron, R. J. Enzyme regulation as an approach to interference with polyamine biosynthesis–an alternative to enzyme inhibition. Adv. Enzyme Regul., *27:* 57–79, 1988.
18. Porter, C. W., Ganis, B., Libby, P. R., and Bergeron, R. J. Correlations between polyamine analogue-induced increases in spermidine/spermine N1-acetyltransferase activity, polyamine pool depletion, and growth inhibition in human melanoma cell lines. Cancer Res, *51:* 3715–3720, 1991.
19. Casero, R. A., Jr., Celano, P., Ervin, S. J., Porter, C. W., Bergeron, R. J., and Libby, P. R. Differential induction of spermidine/spermine N1-acetyltransferase in human lung cancer cells by the bis(ethyl)polyamine analogues. Cancer Res., *49:* 3829–3833, 1989.
20. Pegg, A. E., Wechter, R., Pakala, R., and Bergeron, R. J. Effect of N1, N12-bis(ethyl)spermine and related compounds on growth and polyamine acetylation, content, and excretion in human colon tumor cells. J. Biol. Chem., *264:* 11744–11749, 1989.
21. Kramer, D. L., Fogel-Petrovic, M., Diegelman, P., Cooley, J. M., Bernacki, R. J., McManis, J. S., Bergeron, R. J., and Porter, C. W. Effects of novel spermine analogues on cell cycle progression and apoptosis in MALME-3M human melanoma cells. Cancer Res., *57:* 5521–5527, 1997.
22. Kramer, D. L., Vujcic, S., Diegelman, P., Alderfer, J., Miller, J. T., Black, J. D., Bergeron, R. J., and Porter, C. W. Polyamine analogue induction of the p53–p21WAF1/CIP1-Rb pathway and G1 arrest in human melanoma cells. Cancer Res., *59:* 1278–1286, 1999.
23. Ray, R. M., Zimmerman, B. J., McCormack, S. A., Patel, T. B., and Johnson, L. R. Polyamine depletion arrests cell cycle and induces inhibitors p21(Waf1/Cip1), p27(Kip1), and p53 in IEC-6 cells. Am. J. Physiol., *276:* C684–C691, 1999.
24. Li, L., Li, J., Rao, J. N., Li, M., Bass, B. L., and Wang, J. Y. Inhibition of polyamine synthesis induces p53 gene expression but not apoptosis. Am. J. Physiol., *276:* C946–C954, 1999.
25. Danzin, C., Marchal, P., and Casara, P. Irreversible inhibition of rat S-adenosylmethionine decarboxylase by 5′-([(Z)-4-amino-2-butenyl]methylamino)-5′-deoxyadenosine. Biochem. Pharmacol., *40:* 1499–1503, 1990.
26. O'Connor, P. M., Jackman, J., Bae, I., Myers, T. G., Fan, S., Mutoh, M., Scudiero, D. A., Monks, A., Sausville, E. A., Weinstein, J. N., Friend, S., Fornace, A. J., Jr., and Kohn, K. W. Characterization of the p53 tumor suppressor pathway in cell lines of the National Cancer Institute anticancer drug screen and correlations with the growth-inhibitory potency of 123 anticancer agents. Cancer Res., *57:* 4285–4300, 1997.
27. Krishan, A. Rapid flow cytofluorometric analysis of mammalian cell cycle by propidium iodide staining. J. Cell Biol., *66:* 188–193, 1975.
28. Fredlund, J. O., Johansson, M., Baldetorp, B., and Oredsson, S. M. Abnormal DNA synthesis in polyamine deficient cells revealed by bromodeoxyuridine-flow cytometry technique. Cell Prolif., *27:* 243–256, 1994.
29. Baldetorp, B., Dalberg, M., Holst, U., and Lindgren, G. Statistical evaluation of cell kinetic data from DNA flow cytometry (FCM) by the EM algorithm. Cytometry, *10:* 695–705, 1989.
30. Dimri, G. P., Lee, X., Basile, G., Acosta, M., Scott, G., Roskelley, C., Medrano, E. E., Linskens, M., Rubelj, I., Pereira-Smith, O., and *et al.* A biomarker that identifies senescent human cells in culture and in aging skin *in vivo*. Proc. Natl. Acad. Sci. USA, *92:* 9363–9367, 1995.
31. Chang, B. D., Watanabe, K., Broude, E. V., Fang, J., Poole, J. C., Kalinichenko, T. V., and Roninson, I. B. Effects of p21Waf1/Cip1/Sdi1 on cellular gene expression: implications for carcinogenesis, senescence, and age-related diseases. Proc. Natl. Acad. Sci. USA, *97:* 4291–4296, 2000.
32. Kramer, D. L., Khomutov, R. M., Bukin, Y. V., Khomutov, A. R., and Porter, C. W. Cellular characterization of a new irreversible inhibitor of S-adenosylmethionine decarboxylase and its use in determining the relative abilities of individual polyamines to sustain growth and viability of L1210 cells. Biochem. J., *259:* 325–331, 1989.
33. Stein, G. H., Drullinger, L. F., Robetorye, R. S., Pereira-Smith, O. M., and Smith, J. R. Senescent cells fail to express cdc2, cycA, and cycB in response to mitogen stimulation. Proc. Natl. Acad. Sci. USA, *88:* 11012–11016, 1991.
34. Chin, L., Merlino, G., and DePinho, R. A. Malignant melanoma: modern black plague and genetic black box. Genes Dev., *12:* 3467–3481, 1998.
35. Wu, X., Bayle, J. H., Olson, D., and Levine, A. J. The p53-mdm-2 autoregulatory feedback loop. Genes Dev., *7:* 1126–1132, 1993.
36. Chang, B. D., Xuan, Y., Broude, E. V., Zhu, H., Schott, B., Fang, J., and Roninson, I. B. Role of p53 and p21waf1/cip1 in senescence-like terminal proliferation arrest induced in human tumor cells by chemotherapeutic drugs. Oncogene, *18:* 4808–4818, 1999.
37. Vogt, M., Haggblom, C., Yeargin, J., Christiansen-Weber, T., and Haas, M. Independent induction of senescence by p16INK4a and p21CIP1 in spontaneously immortalized human fibroblasts. Cell Growth Differ. *9:* 139–146, 1998.
38. Fang, L., Igarashi, M., Leung, J., Sugrue, M. M., Lee, S. W., and Aaronson, S. A. p21Waf1/Cip1/Sdi1 induces permanent growth arrest with markers of replicative senescence in human tumor cells lacking functional p53. Oncogene, *18:* 2789–2797, 1999.
39. Campisi, J. The role of cellular senescence in skin aging. J. Investig. Dermatol. Symp. Proc., *3:* 1–5, 1998.
40. Medrano, E. E., Yang, F., Boissy, R., Farooqui, J., Shah, V., Matsumoto, K., Nordlund, J. J., and Park, H. Y. Terminal differentiation and senescence in the human melanocyte: repression of tyrosine-phosphorylation of the extracellular signal-regulated kinase 2 selectively defines the two phenotypes. Mol. Biol. Cell, *5:* 497–509, 1994.
41. Chang, B. D., Broude, E. V., Dokmanovic, M., Zhu, H., Ruth, A., Xuan, Y., Kandel, E. S., Lausch, E., Christov, K., and Roninson, I. B. A senescence-like phenotype distinguishes tumor cells that undergo terminal proliferation arrest after exposure to anticancer agents. Cancer Res., *59:* 3761–3767, 1999.
42. Chang, B. D., Broude, E. V., Fang, J., Kalinichenko, T. V., Abdryashitov, R., Poole, J. C., and Roninson, I. B. p21Waf1/Cip1/Sdi1-induced growth arrest is associated with depletion of mitosis-control proteins and leads to abnormal mitosis and endoreduplication in recovering cells. Oncogene, *19:* 2165–2170, 2000.
43. Bravard, A., Petridis, F., and Luccioni, C. Modulation of antioxidant enzymes p21WAF1 and p53 expression during proliferation and differentiation of human melanoma cell lines. Free Radic. Biol. Med., *26:* 1027–1033, 1999.
44. Gartel, A. L., Ye, X., Goufman, E., Shianov, P., Hay, N., Najmabadi, F., and Tyner, A. L. Myc represses the p21(WAF1/CIP1) promoter and interacts with Sp1/Sp3. Proc. Natl. Acad. Sci. USA, *98:* 4510–4515, 2001.
45. Celano, P., Baylin, S. B., Giardiello, F. M., Nelkin, B. D., and Casero, R. A., Jr. Effect of polyamine depletion on c-myc expression in human colon carcinoma cells. J. Biol. Chem., *263:* 5491–5494, 1988.
46. el-Deiry, W. S., Tokino, T., Velculescu, V. E., Levy, D. B., Parsons, R., Trent, J. M., Lin, D., Mercer, W. E., Kinzler, K. W., and Vogelstein, B. WAF1, a potential mediator of p53 tumor suppression. Cell, *75:* 817–825, 1993.
47. Wang, J. Y., Viar, M. J., Li, J., Shi, H. J., Patel, A. R., and Johnson, L. R. Differences in transglutaminase mRNA after polyamine depletion in two cell lines. Am. J. Physiol., *274:* C522–C530, 1998.
48. West, M. D., Shay, J. W., Wright, W. E., and Linskens, M. H. Altered expression of plasminogen activator and plasminogen activator inhibitor during cellular senescence. Exp. Gerontol., *31:* 175–193, 1996.
49. Hiraiwa, M., Taylor, E. M., Campana, W. M., Darin, S. J., and O'Brien, J. S. Cell death prevention, mitogen-activated protein kinase stimulation, and increased sulfatide concentrations in Schwann cells and oligodendrocytes by prosaposin and prosaptides. Proc. Natl. Acad. Sci. USA, *94:* 4778–4781, 1997.
50. Akahani, S., Nangia-Makker, P., Inohara, H., Kim, H. R., and Raz, A. Galectin-3: a novel antiapoptotic molecule with a functional BH1 (NWGR) domain of Bcl-2 family. Cancer Res., *57:* 5272–5276, 1997.
51. Fujimura, M., Morita-Fujimura, Y., Kawase, M., Copin, J. C., Calagui, B., Epstein, C. J., and Chan, P. H. Manganese superoxide dismutase mediates the early release of mitochondrial cytochrome C and subsequent DNA fragmentation after permanent focal cerebral ischemia in mice. J. Neurosci., *19:* 3414–3422, 1999.
52. Migliaccio, E., Giorgio, M., Mele, S., Pelicci, G., Reboldi, P., Pandolfi, P. P., Lanfrancone, L., and Pelicci, P. G. The p66shc adaptor protein controls oxidative stress response and life span in mammals. Nature (Lond.), *402:* 309–313, 1999.
53. Adler, M. J., Coronel, C., Shelton, E., Seegmiller, J. E., and Dewji, N. N. Increased gene expression of Alzheimer disease β-amyloid precursor protein in senescent cultured fibroblasts. Proc. Natl. Acad. Sci. USA, *88:* 16–20, 1991.